

UPDATED ELECTRON-CONDUCTION OPACITIES: THE IMPACT ON LOW-MASS STELLAR MODELS

S. CASSISI,¹ A. Y. POTEKHIN,² A. PIETRINFERNI,¹ M. CATELAN,³ & M. SALARIS⁴

Received 2007 January 18; accepted 2007 February 28

ABSTRACT

We review the theory of electron-conduction opacity, a fundamental ingredient in the computation of low-mass stellar models; shortcomings and limitations of the existing calculations used in stellar evolution are discussed. We then present new determinations of the electron-conduction opacity in stellar conditions for an arbitrary chemical composition, that improve over previous works and, most importantly, cover the whole parameter space relevant to stellar evolution models (i.e., both the regime of partial and high electron degeneracy). A detailed comparison with the currently used tabulations is also performed. The impact of our new opacities on the evolution of low-mass stars is assessed by computing stellar models along both the H- and He-burning evolutionary phases, as well as Main Sequence models of very low-mass stars and white dwarf cooling tracks.

Subject headings: conduction – stars: horizontal-branch – white dwarfs – stars: interiors – stars: evolution

1. INTRODUCTION

One of the main physical inputs required to solve the equations of stellar structure is the electron thermal conductivity. When the degree of electron degeneracy is significant, electron conduction is the dominant energy transport mechanism, and the value of the electron-conduction opacity – proportional to the inverse of the electron thermal conductivity – enters the equation of the temperature gradient. This physical condition is verified in the interiors of brown dwarfs, very low-mass stars with mass $M_{\text{tot}} < 0.15M_{\odot}$ (the exact value slightly affected by the metal content; see Chabrier & Baraffe 2000 for a review), in the He-core of low-mass stars during their Red Giant Branch (RGB) evolution (see, e.g., Salaris, Cassisi, & Weiss 2002), in the CO core of Asymptotic Giant Branch stars, as well as in white dwarfs (inside the core and in a portion of the envelope – see, e.g., Prada Moroni & Straniero 2002) and envelopes of neutron stars.

Until the mid-1990s, the main sources of electron-conduction opacity for stellar model computations were those provided by Hubbard & Lampe (1969), by Itoh and coworkers (Flowers & Itoh 1976, 1979, 1981; Itoh et al. 1983, 1984; Mitake, Ichimaru, & Itoh 1984; Itoh & Kohyama 1993; Itoh, Hayashi, & Kohyama 1993), and by Yakovlev and coworkers (Yakovlev & Urpin 1980; Urpin & Yakovlev 1980; Raikh & Yakovlev 1982; Yakovlev 1987; Baiko & Yakovlev 1995). Each of these sources of opacities has its own shortcomings. The Hubbard & Lampe tabulations cover a very limited set of element mixtures, do not take into account relativistic effects, and contain significant gaps in the temperature-density diagram (see § 2.3 below). The formulae by Itoh et al. (1983, 1984,

1993) and Itoh & Kohyama, as well as Yakovlev & Urpin, Raikh & Yakovlev, and Baiko & Yakovlev, are successive improvements – in their domains of validity – over the Hubbard & Lampe results for the opacity contribution due to electron-ion (*ei*) scattering: they take into account relativistic effects, more accurate structure factors for an ion liquid, phonon-electron interactions for an ion solid, and can be employed to compute conductive opacities for arbitrary chemical mixtures. Simple formulae for the electron-electron (*ee*) scattering contribution to the conductive opacities have been derived by Urpin & Yakovlev (1980) and Potekhin, Chabrier, & Yakovlev (1997). However, the above-cited results by Itoh's and Yakovlev's groups are applicable only when electrons are strongly degenerate ($T \ll T_{\text{F}}$, where T_{F} is the Fermi temperature) a condition which is not strictly satisfied in RGB stars (see, e.g., Fig. 18 in Catelan 2005). In addition, they do not take into account important collective plasma effects near the solid-liquid phase transition (Baiko et al. 1998). These effects have been taken into account by Potekhin et al. (1999), whose calculations can be also used to compute opacities for arbitrary astrophysical mixtures at $T \ll T_{\text{F}}$. For the *ei* scattering contribution, the latter calculations have been extended to partially degenerate plasmas by Ventura & Potekhin (2001), using a thermal averaging procedure presented by Potekhin (1999) (see § 2.3 below).

The value of the electron-conduction opacity is crucial in particular for the evolution of low-mass RGB stars and the fate of their progeny (see, e.g., the extensive discussions in Catelan 2005 and Catelan, de Freitas Pacheco, & Horvath 1996). The whole thermal stratification inside the He-core and the temperature at the base of the surrounding H-burning shell depend strongly on the efficiency of electron conduction (for a detailed discussion on this issue see Catelan et al. 1996; Salaris et al. 2002, and references therein). As a consequence, the mass size of the He core (M_{cHe}) at the He-burning ignition (the He-flash at the RGB tip) depends on the value of the electron conductivity. An accurate determination of the M_{cHe} value is extremely important for several astrophysical problems. First of all, the value of M_{cHe} regulates the

¹ INAF – Osservatorio Astronomico di Teramo, via M. Maggini s.n., 64100 Teramo, Italy; e-mail: cassisi, pietrinforni@oa-teramo.inaf.it

² Ioffe Physico-Technical Institute, Politeknicheskaya 26, 194021 St. Petersburg, Russia; e-mail: palex@astro.ioffe.ru

³ Pontificia Universidad Católica de Chile, Departamento de Astronomía y Astrofísica, Av. Vicuña Mackenna 4860, 782-0436 Macul, Santiago, Chile; e-mail: mcatelan@astro.puc.cl

⁴ Astrophysics Research Institute, Liverpool John Moores University, Twelve Quays House, Birkenhead, CH41 1LD, UK; e-mail: ms@astro.livjm.ac.uk

stellar luminosity at the RGB tip and, in turn, the evolutionary lifetime along the RGB: any increase of M_{cHe} causes an increase in both the surface luminosity at the RGB tip and the RGB evolutionary lifetime. Given that the mass loss efficiency along the RGB increases with increasing surface luminosity and decreasing effective temperature (see, e.g., Reimers 1975) the amount of mass lost during the RGB evolution is strongly influenced by any variation in the mass of the He core at the He-flash. This has a sizeable effect on the morphology of the Horizontal Branch (HB) (see the review by Renzini & Fusi Pecci 1988 for a detailed discussion on this issue). In addition, one has to notice that the brightness of the RGB tip is a commonly used standard candle for old, metal-poor stellar systems (Lee, Freedman, & Madore 1993). Changes in the theoretical predictions of M_{cHe} have a direct influence on the theoretical calibration of this distance indicator and, in turn, on the derived distances (Salaris & Cassisi 1998). Also, the luminosity of the core He-burning phase in low-mass stars is mainly controlled by the value of M_{cHe} . Given that the HB luminosity and, in particular, the mean brightness of RR Lyrae stars is one of the most important distance indicators for old stellar systems, the theoretical calibration of this standard candle depends on the accuracy of the electron-conduction opacities.

The value of M_{cHe} also affects the duration of the core He-burning phase, playing therefore a role in the theoretical calibration of the so-called R -parameter (number ratio of HB stars to RGB stars brighter than the HB), which is an indicator of the initial He content of old stellar populations (Iben 1968). When using the Itoh et al. conductive opacities, Castellani & Degl’Innocenti (1999) found an increase by $\sim 0.005 M_{\odot}$ of M_{cHe} at the He flash for a $0.8 M_{\odot}$ star with metallicity $Z = 2 \times 10^{-4}$ compared to models based on the Hubbard & Lampe (1969) opacities. The same numerical experiment performed on a $1.5 M_{\odot}$ star with initial solar composition showed an increase of $\sim 0.008 M_{\odot}$. A similar comparison performed with the Potekhin et al. (1999) opacities provides He-core masses at the He-ignition between those obtained with the Itoh et al. and the Hubbard & Lampe ones, but closer to the Itoh et al. results.

The above-cited papers by Itoh et al., Yakovlev et al., and Potekhin et al. were devoted mostly to plasmas at the conditions typical for neutron star envelopes, where ee scattering is relatively unimportant. Therefore the ee scattering mechanism was paid little attention in those papers. For instance, Potekhin et al. (1997, 1999) used a fitting formula for the ee contribution, valid only for strongly degenerate electrons. However, as already noted by Hubbard & Lampe (1969) and recently stressed by Catelan (2005), the ee scattering can give a considerable contribution to the opacity in partially degenerate regions within the He-core of RGB stars. In this paper we improve the treatment by Potekhin et al. (1999) and Potekhin (1999) for the case of a non-magnetized plasma by including the ee scattering in partially degenerate and nondegenerate matter. In addition, we take into account a recent improvement of the treatment of the ee scattering in degenerate matter by Shternin & Yakovlev (2006). To verify the impact of these new conductive opacities, we compute models of low-mass stars and perform a detailed analysis of the effects of the new conductive opac-

ity evaluations on both the RGB and HB evolutionary phases. We also assess their impact on models of very low-mass stars and white dwarfs.

The paper is organized as follows: in § 2 we briefly discuss the physical mechanisms governing the electron conduction in the different physical regimes and emphasize the assumptions made by the various existing treatments – including our new updated results – with the aim of highlighting the limitations of the available tabulations of conductive opacities. An analysis of the impact of our new conductive opacities on stellar models is presented in § 3. A summary and final remarks follow in § 4.

2. STELLAR CONDUCTIVE OPACITIES: THE STATE-OF-THE-ART

Let us recall that the total opacity of stellar matter (e.g., Marshak 1940; Carson 1976) can be written as $\kappa_{\text{total}} = 1/(\kappa_{\text{rad}}^{-1} + \kappa_{\text{c}}^{-1})$, where κ_{rad} and κ_{c} are the radiative and conductive opacities, respectively. The latter is related to the thermal conductivity \varkappa by the equation

$$\kappa_{\text{c}} = \frac{16\sigma T^3}{3\rho\varkappa}, \quad (1)$$

where σ is the Stefan-Boltzmann constant, T is the temperature, and ρ is the density.

The kinetic method (Ziman 1960) is most practical for calculating \varkappa . Using the elementary theory in which the effective electron scattering rate ν does not depend on the electron velocity, one can write (Ziman 1960)

$$\varkappa = a \frac{n_e k^2 T}{m_e \nu}, \quad (2)$$

where n_e is the electron number density, m_e is the electron mass, k is the Boltzmann constant, $a = 3/2$ for a nondegenerate electron gas ($T \gg T_{\text{F}}$), and $a = \pi^2/3$ for strongly degenerate electrons ($T \ll T_{\text{F}}$). If the electrons are degenerate and relativistic, one should replace m_e in Eq. (2) by $m_e^* = m_e \gamma_{\text{r}}$, where $\gamma_{\text{r}} = \sqrt{1 + x_{\text{r}}^2}$,

$$x_{\text{r}} = p_{\text{F}}/m_e c = 0.01009(\rho Z_i/A)^{1/3} \quad (3)$$

is the relativistic density parameter, $p_{\text{F}} = \hbar(3\pi^2 n_e)^{1/3}$ is the Fermi momentum, Z_i and A are the nuclear charge and mass numbers, and the mass density ρ is expressed in g cm^{-3} . Note that the electron Fermi temperature that accounts for relativistic effects can be expressed as

$$T_{\text{F}} = (m_e^* - m_e)c^2/k = 5.93 \times 10^9 \text{ K} (\gamma_{\text{r}} - 1), \quad (4)$$

where k is the Boltzmann constant.

In a fully ionized plasma, ν is determined by electron-ion and electron-electron Coulomb collisions. Let us assume that the effective frequencies of different kinds of collisions simply add up, i.e., $\nu = \nu_{ei} + \nu_{ee}$. This so-called *Matthiessen rule* is strictly valid only for extremely degenerate electrons (see Hubbard & Lampe 1969). However, in practice it gives a good estimate of the conductivity: one can show that $\nu_{ei} + \nu_{ee} \leq \nu \leq \nu_{ei} + \nu_{ee} + \delta\nu$, where $\delta\nu \ll \min(\nu_{ei}, \nu_{ee})$ (see Ziman 1960).

2.1. Nondegenerate Electron Gas

Let us consider first the case where the electrons are non-degenerate ($T \gg T_{\text{F}}$) and non-relativistic ($x_{\text{r}} \ll 1$).

This case has been studied, e.g., by Spitzer & Härm (1953), Braginskii (1958), and Spitzer (1962). The effective *energy-averaged* ei collision frequency is

$$\nu_{ei} = \frac{4}{3} \sqrt{\frac{2\pi}{m_e}} \frac{Z_i^2 e^4}{(kT)^{3/2}} n_i \Lambda_{ei}, \quad (5)$$

where n_i is the ion number density, m_i is the ion mass, and Λ_{ei} is the so-called Coulomb logarithm. In the considered case Λ_{ei} is a slowly varying function of density and temperature. In general, its value depends on the approximations used to solve the Boltzmann equation, but in any case its order-of-magnitude estimate is given by the elementary theory, where the Coulomb collision integral is truncated at small and large impact parameters of the electrons. Then one obtains $\Lambda_{ei} \sim \ln(r_{\max}/r_{\min})$, where r_{\max} and r_{\min} are the maximum and minimum electron impact parameters. The parameter r_{\max} can be set equal to the Debye screening length, $r_{\max}^{-2} = 4\pi(n_e + Z_i^2 n_i)e^2/kT$. The second parameter can be estimated as $r_{\min} = \max(\lambda_T, r_{cl})$, where $\lambda_T = \sqrt{2\pi\hbar^2/m_e kT}$ is the thermal de Broglie wavelength, which limits r_{\min} in the high-temperature regime (where the Born approximation holds), and $r_{cl} = Z_i e^2/kT$ is the classical closest-approach distance of a thermal electron, which limits r_{\min} in the low-temperature, quasiclassical regime.

A similar effective frequency

$$\nu_{ee} = \frac{8}{3} \sqrt{\frac{\pi}{m_e}} \frac{e^4}{(kT)^{3/2}} n_e \Lambda_{ee} \quad (6)$$

characterizes the efficiency of ee collisions. If $\Lambda_{ee} \sim \Lambda_{ei}$, then $\nu_{ei}/\nu_{ee} \sim Z_i$, therefore for large Z_i the ei collisions are much more efficient than the ee collisions.

2.2. Strongly Degenerate Electrons

The thermal conductivity of strongly degenerate electrons in a fully ionized plasma is given by Eq. (2) with $a = \pi^2/3$. In order to determine the effective collision frequency ν that enters this equation, we shall use the Matthiessen rule, mentioned above. This will allow us to consider the different types of electron scatterings separately in the following sections, and calculate ν as their sum.

2.2.1. Electron-Ion Scattering

Thermal transport coefficients of degenerate electrons were studied in a number of papers. In the 1990's, the formulae for conductive opacities mostly used in astrophysics were those derived by Itoh and coworkers and by Yakovlev and coworkers (see references in §1). These formulae are valid for degenerate electrons in strongly coupled ion liquids or solids – i.e., at $T \ll T_F$ and $\Gamma > 1$, where

$$\Gamma = \frac{(Z_i e)^2}{a_i k T} = \frac{0.2275}{T_6} Z_i^2 \left(\frac{\rho}{A}\right)^{1/3} \quad (7)$$

is the Coulomb coupling parameter⁵ (here $a_i = [4\pi n_i/3]^{-1/3}$ is the ion sphere radius, $T_6 = T/10^6$ K, and ρ is expressed in g cm^{-3}).

⁵ This parameter regulates the state of the Coulomb plasma: the ions constitute a gas at $\Gamma \lesssim 1$, a liquid at $1 \lesssim \Gamma < \Gamma_m$, and a crystal at $\Gamma > \Gamma_m$, where $\Gamma_m \approx 175$ (see, e.g., Potekhin & Chabrier 2000).

It is convenient to present the effective frequency of ei collisions in the form

$$\nu_{ei} = \frac{4\pi Z_i^2 e^4}{p_F^2 v_F} n_i \Lambda_{ei} \quad (8)$$

(where $v_F = p_F/m_e^* = cx_r/\gamma_r$ is the electron Fermi velocity), and derive a fitting formula for the Coulomb logarithm Λ_{ei} as a function of n_e , T , and Z_i . Yakovlev & Urpin (1980) used Eq. (8) in the ion liquid regime, where Λ_{ei} is a slow function of order unity. They employed another form of ν_{ei} for an ion crystal, where collective effects are important – that is, where electrons are scattered not by individual ions, but by their collective excitations, the phonons.

However, Baiko et al. (1998) showed that in fully ionized dense plasmas there is no appreciable discontinuity between the conductivities in the solid and liquid phases. This is due to the incipient long-range ion structures in the ion liquid and multiphonon scattering in the solid near the melting point $\Gamma \sim \Gamma_m$. Thus, the conductivity is smooth across the melting. More recent and more accurate calculations (Potekhin et al. 1999) resulted in new fitting formulae for the ei conductive opacities in degenerate matter. These calculations included the accurate numerical structure factor for a Coulomb liquid calculated by F. Rogers & H. E. DeWitt (unpublished) and fitted by Young, Corey, & DeWitt (1991), for a Coulomb coupling parameter $\Gamma \geq 1$. Potekhin et al. (1999) have taken account of the modifications of the *effective* (for electron scattering) ion structure factor around the melting point, discussed by Baiko et al., as well as the quantization of ion motion at T below the ion plasma temperature $T_{p,\text{ion}}$ and “freezing-out” of the umklapp processes at $T \ll T_{p,\text{ion}}$ (Raikh & Yakovlev 1982). A correct limiting form of the ion structure factor at $\Gamma \ll 1$ was also ensured. Hence the results of Potekhin et al. (1999) are probably valid at any Γ . On the other hand, it should be noted that rigorous calculations for $\Gamma \lesssim 1$ have never been carried out, and would certainly prove of interest in placing this “smooth interpolation argument” on a more solid physical basis.

The absence of a big discontinuity at $\Gamma = \Gamma_m$ allowed Potekhin et al. (1999) to construct a single fitting formula for Λ_{ei} using Eq. (8) at all temperatures. We shall follow this approach hereafter. It should be noted, however, that Λ_{ei} in Eq. (8) is a slowly varying function only at $\Gamma \lesssim \Gamma_m$, but it rapidly decreases in the solid regime at $\Gamma \gg \Gamma_m$ (see Potekhin et al. 1999 for details).

2.2.2. Electron-Electron Scattering

The expression of ν_{ee} for the relativistic degenerate electrons at $T \ll T_p$ was obtained by Flowers & Itoh (1976). Here $T_p = \hbar\omega_p/k$ is the electron plasma temperature, determined by the electron plasma frequency $\omega_p = \sqrt{4\pi e^2 n_e/m_e^*}$. Urpin & Yakovlev (1980) extended the results of Flowers & Itoh (1976) to higher temperatures, where $T \ll T_F$, but not necessarily $T \ll T_p$. Potekhin et al. (1997, 1999) calculated ee conductive opacities according to the theory of Urpin & Yakovlev (1980) and presented a fitting formula for their results.

Recently, Shternin & Yakovlev (2006) have reconsidered the problem taking into account the Landau damping of transverse plasmons. This effect is due to the

difference of the components of the polarizability tensor, responsible for screening the charge-charge and current-current interactions: the transverse current-current interactions undergo “dynamical screening.” It was neglected by Urpin & Yakovlev (1980) but later studied by Heiselberg & Pethick (1993) in the context of the transport coefficients of the quark-gluon plasma. Shternin & Yakovlev showed that the Landau damping of transverse plasmons strongly increases ν_{ee} in the domain of $x_r \gtrsim 1$ and $T \ll T_p$. Their result can be written as

$$\nu_{ee} = \frac{m_e c^2}{\hbar} \frac{6\alpha_f^{3/2}}{\pi^{5/2}} x_r y \sqrt{\beta_r} I(\beta_r, y), \quad (9)$$

where α_f is the fine-structure constant, $\beta_r = v_F/c = x_r/\gamma_r$, $y = \sqrt{3} T_p/T = (571.6/T_6)\sqrt{\beta_r} x_r$, and

$$\begin{aligned} I(\beta, y) &= \frac{1}{\beta} \left(\frac{10}{63} - \frac{8/315}{1 + 0.0435y} \right) \\ &\times \ln \left(1 + \frac{128.56}{37.1y + 10.83y^2 + y^3} \right) \\ &+ \beta^3 \left(\frac{2.404}{B} + \frac{C - 2.404/B}{1 + 0.1\beta y} \right) \\ &\times \ln \left[1 + \frac{B}{A\beta y + (\beta y)^2} \right] \\ &+ \frac{\beta}{1 + D} \left(C + \frac{18.52\beta^2 D}{B} \right) \\ &\times \ln \left[1 + \frac{B}{Ay + 10.83(\beta y)^2 + (\beta y)^{8/3}} \right], \quad (10) \end{aligned}$$

where $A = 12.2 + 25.2\beta^3$, $B = A \exp[(0.123636 + 0.016234\beta^2)/C]$, $C = 8/105 + 0.05714\beta^4$, and $D = 0.1558 y^{1-0.75\beta}$.

These equations are valid only for $T \ll T_F$; their extension to the case $T \gtrsim T_F$ will be suggested in §2.3.

It is easy to check that Eqs. (9) and (10) reproduce the low-density ($x_r \ll 1$) asymptote of the previous fit to ν_{ee} presented by Potekhin et al. (1997, 1999). However, the deviation from the previous results is already large at $x_r \sim 1$ and can reach many orders of magnitude at $x_r \gg 1$.

2.2.3. Impurities and Mixtures

Real stellar plasmas are often mixtures of different chemical elements. In this case Eq. (3) for the relativity parameter x_r has to be modified by replacing Z_i/A by the unweighted mean value of the charge-to-mass ratio, $\langle Z_i/A \rangle$, averaged over all species. The effective collision frequency ν_{ei} should also be modified. The required modification can be different, depending on the state of the plasma and on the amount of impurities. For example, Flowers & Itoh (1976), Yakovlev & Urpin (1980), and Itoh & Kohyama (1993) considered electron scattering by charged impurities in a Coulomb crystal. If the fraction of impurities is small and they are randomly distributed, electron-impurity scattering can be treated as scattering by charge fluctuations, controlled by the impurity parameter $Q = \sum_j Y_j (Z_j - \langle Z \rangle)^2$, where $Y_j = n_j / \sum_j n_j$ is the number fraction of impurities of the j th kind, Z_j is their charge number, and $\langle Z \rangle$ is the mean charge number, which in the considered case is close to the charge number of the main ion species that forms the crystal lattice.

Then, using the Matthiessen rule, one can obtain ν_{ei} as a sum of the terms corresponding to the ei (electron-phonon) scattering in a homogeneous lattice and to the electron scattering by charge fluctuations, which is given by Eq. (8) with Z_i replaced by $Z_{\text{imp}} = \sqrt{Q}$. This approach has been adopted by Yakovlev & Urpin (1980), Potekhin & Yakovlev (1996), and Gnedin, Yakovlev, & Potekhin (2001), and implemented in the online database referenced below.

An alternative approach is relevant when there is no dominant ion species which forms a crystal (e.g., in a liquid, a gas, or a glassy alloy). In this case, one can use Eq. (8) with $Z_i^2 n_i \Lambda_{ei}$ replaced by $\sum_j Z_j^2 n_j \Lambda_{ei}^j$, where summation is over all ion species j , and the Coulomb logarithm Λ_{ei}^j depends generally on j . An approximation to Λ_{ei}^j based on the plasma “additivity rule” has been suggested by Potekhin et al. (1999). A much simpler yet reasonable approximation to the conductive opacity can be obtained by using an effective charge number equal to $\sqrt{\langle Z^2 \rangle} \equiv (\sum_j Z_j^2 n_j)^{1/2}$.

A brief discussion and comparison of the two approaches has been given by Brown, Bildsten, & Chang (2002).

In the present paper, we consider pure He composition for the core of RGB stellar models. This is justified by low metallicities in most of these models, which make the exact conductivity of a mixture close to the pure He conductivity. For instance, an admixture of 0.1% (by number) of N or C to the He liquid raises the conductive opacity by $\approx 1\%$, which can be safely neglected.

2.3. Partially Degenerate Electrons

The thermal conductivity of partially degenerate electrons is more difficult to calculate. For the fully ionized Coulomb plasmas this problem was studied by Lampe (1968), who calculated the transport coefficients of a weakly coupled plasma of nondegenerate ions and partially degenerate nonrelativistic electrons by means of a Chapman-Enskog solution of the quantum Lenard-Balescu kinetic equation, including both ee and ei collisions. The employed method is more fundamental and accurate than the simple estimates presented in Sect. 2.1. However, the ion correlations have not been taken into account, i.e., $\Gamma \ll 1$ was assumed. Hubbard & Lampe (1969) combined these calculations with earlier results of Hubbard (1966), who considered the transport coefficients determined by the ei collisions in a nonrelativistic degenerate electron gas, taking into account ion-ion correlations. Hubbard & Lampe provided conductive opacities in tabular form for various chemical compositions.

In the domains of degenerate electrons and strongly correlated ions, more accurate results have been obtained after the work of Hubbard & Lampe (1969), as discussed in Sect. 2.2. Although the Hubbard & Lampe results are sufficiently accurate at $T \gg T_F$, their tabular form of presentation does not allow their extension to other chemical compositions or plasma parameters beyond the tabulated range.

Potekhin (1999) proposed a procedure of averaging the expressions for ei transport coefficients, obtained in the limit $T/T_F \rightarrow 0$, over the thermal distribution of the electron energies. Although this procedure was originally devised for taking account of thermal broadening of os-

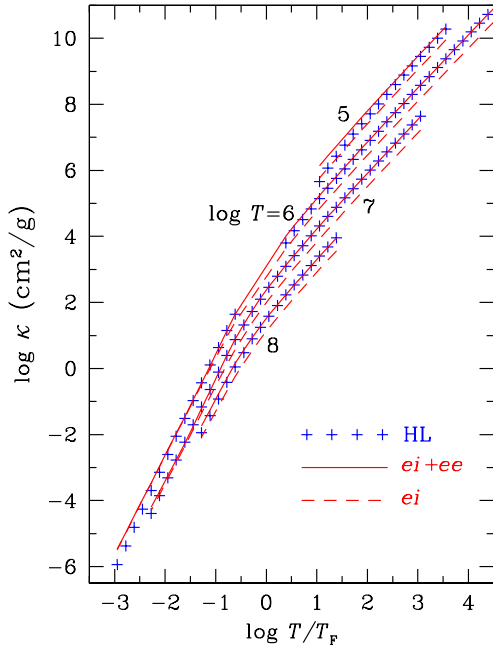


FIG. 1.— Conductive opacity ($\kappa \equiv \kappa_c = \kappa_{ei} + \kappa_{ee}$) of helium as a function of the degeneracy parameter T/T_F : comparison of Hubbard & Lampe (1969) data (*crosses*) with the present *ei + ee* results (*solid lines*) and with the *ei* opacities (*dashed lines*) for values of $\log T$ (K) marked near the lines.

cillations of the transport coefficients in quantizing magnetic fields at $T \ll T_F$, it was shown to reproduce also the correct non-magnetic limit of \varkappa at $T \gg T_F$ (Ventura & Potekhin 2001). According to this recipe,

$$\varkappa = k^2 T (\sigma_2 - \sigma_1^2 / \sigma_0), \quad (11)$$

where

$$\sigma_n = \int \frac{\chi^n}{\nu_{ei}(\epsilon)} \frac{\mathcal{N}(\epsilon)}{m_e^*(\epsilon)} \frac{e^\chi}{(e^\chi + 1)^2} d\chi, \quad (12)$$

ϵ is the electron energy, $\chi = (\epsilon - \mu)/kT$, μ is the electron chemical potential, $\mathcal{N}(\epsilon)$ is the number density of electron states with energies smaller than ϵ (i.e., the electron number density that would correspond to the Fermi energy ϵ at $T = 0$), and $\nu_{ei}(\epsilon)$ is the effective collision frequency of electrons with energy ϵ . In a nonquantizing (or zero) magnetic field, $\mathcal{N}(\epsilon) = p^3/(3\pi^2\hbar^3)$ and $m_e^*(\epsilon) = \sqrt{m_e^2 + (p/c)^2}$, where p is the electron momentum.

We adopt this approach to the *ei* opacity calculations at arbitrary T/T_F .

There is no such procedure for the *ee* collisions. Note that a correct expression for ν_{ee} must reproduce the general dependence (6) at very high T or very low ρ (maybe up to a factor of a few, given the logarithmic accuracy of the estimates of Λ in §2.1). In particular, Eq. (6) implies $\nu_{ee} \propto T^{-3/2} \ln T$ at $T \rightarrow \infty$, which agrees with an accurate asymptote at $T \gg T_F$ obtained by R. H. Williams & H. E. DeWitt (1968, unpublished) and reproduced by Eq. (16) of Lampe (1968). In contrast, the fit (10), being substituted into Eq. (9), produces a formal asymptote $\nu_{ee} \propto T^{-1} \ln T$ at $T \rightarrow \infty$. Clearly, Eq. (10) must be corrected at $T \gtrsim T_F$.

We construct such a correction, using the numerical data published by Hubbard & Lampe (1969), in such

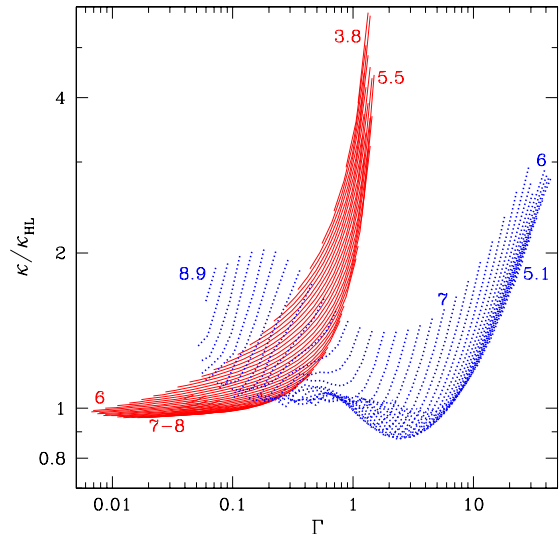


FIG. 2.— Ratio of our new conductive opacities to Hubbard & Lampe (1969) data for helium as a function of the ion Coulomb coupling parameter Γ for $10^{3.8} \leq T(\text{K}) < 10^9$. Each line corresponds to a constant T value. *Solid lines*: nondegenerate matter; *dotted lines*: degenerate matter. Numbers near some of the curves are the corresponding values of $\log T$ (K).

a way as to reproduce their tabulated conductivities in those $\rho - T$ domains where their data can be trusted (see below). Specifically, we propose the following interpolation formula⁶ for the case of arbitrary degeneracy:

$$\nu_{ee} = \nu_{ee}^{\text{deg}} \frac{1 + t^2}{1 + t + bt^2 \sqrt{T/T_F}}, \quad (13)$$

where $t = 25T/T_F$, and ν_{ee}^{deg} is given by Eqs. (9) and (10). The coefficient $b = 135/\sqrt{32\pi^7} \approx 0.434$ corresponds to the ratio of the exact limiting expressions at $T \ll T_F$ and $T \gg T_F$ (e.g., Eqs. (16) and (17) of Lampe 1968).

This approximation is compared to the numerical tables of Hubbard & Lampe (1969) for helium in Figs. 1 and 2. The agreement is good at $T \gg T_F$. In Fig. 1 we also show the opacities calculated without taking *ee* scattering into account (the dashed lines). In this case, there is a noticeable difference at $T > T_F$.

In Fig. 2 the solid and dotted lines correspond to the two parts of the Hubbard & Lampe (1969) tables: for weakly ($T/T_F > 1.7$) and strongly ($T/T_F < 1.7$) degenerate electrons, respectively. We have chosen this division because, for many T values, their tables consist of two disconnected parts, which merge roughly at $T/T_F \gtrsim 1.7$. Figure 2 shows that there are two domains of strong disagreement between our opacities and Hubbard & Lampe's at $\Gamma \gtrsim 1$. These deviations take place near the $\rho - T$ domains excluded from the Hubbard & Lampe tables because either the ions are strongly coupled, or their motion is quantized. In these cases the Hubbard & Lampe theory breaks down, therefore this disagreement does not invalidate Eq. (13). An additional disagreement at $\Gamma \gtrsim 1$ and relatively low temperatures comes from the correction by Shternin & Yakovlev (2006), discussed above.

⁶ This represents an improvement over the formula used recently by Barriga-Carrasco & Potekhin (2006).

2.4. Summary of Recent Updates of the Conductive Opacities

From the preceding discussion it is clear that the previous conductive opacity evaluations had the following limitations.

- Formulae by Itoh et al. (1983, 1984, 1993) and Potekhin et al. (1999) are relevant only at strong degeneracy, $T \ll T_F$. This condition is violated in the outer parts of RGB cores (Catelan 2005).
- Itoh et al. (1983) relied on the ion structure factor calculations at $\Gamma > 1$. The condition $\Gamma > 1$ is also violated in some parts of RGB stars (Catelan et al. 1996; Catelan 2005). However, Potekhin et al. (1999) used more accurate evaluations of the ion structure factor at $\Gamma \geq 1$ and an interpolation at $\Gamma < 1$, which allowed them to consider conductivities at arbitrary Γ in spite of the fact that detailed calculations for $\Gamma \lesssim 1$ have not yet been carried out.

In addition, Potekhin et al. (1999) have taken account of multiphonon scattering and incipient long-range order around the melting line ($\Gamma = \Gamma_m$) on the plasma phase diagram (Baiko et al. 1998), which led to a considerable correction to the opacities at $\Gamma \sim 100 - 300$, compared to Itoh et al. results.

- Potekhin (1999) employed a specific thermal averaging for the contribution of the ei scattering to the conductive opacity (§ 2.3), implemented it in subsequent papers (e.g., Ventura & Potekhin 2001; Gnedin et al. 2001), and created an online database for computing the updated electrical and thermal plasma conductivities.⁷ This allows one to compute conductivities determined by ei scattering at arbitrary degeneracy.

However, the absence of a similar thermal averaging procedure for the ee scattering prevented one from obtaining accurate results in the case where the ee scattering can be important. In the conductivity database, two ways were employed previously to extend the non-magnetic opacities beyond the domain of $T \ll T_F$: (A) to ignore ee scattering altogether, or (B) to continue using the theory by Urpin & Yakovlev (1980). Model A was employed in the table of opacities and model B in the Fortran program presented in the database (the latter model was used in the analysis by Catelan 2005).

- In model B the treatment of the ee scattering was based on the old theory of Flowers & Itoh (1976) and Yakovlev & Urpin (1980). As stressed in § 2.2.2, the theory has been considerably improved recently by Shternin & Yakovlev (2006).

In the present paper, we have done the following improvements to the previous treatments of the contribution to the conductive opacity due to the ee scattering:

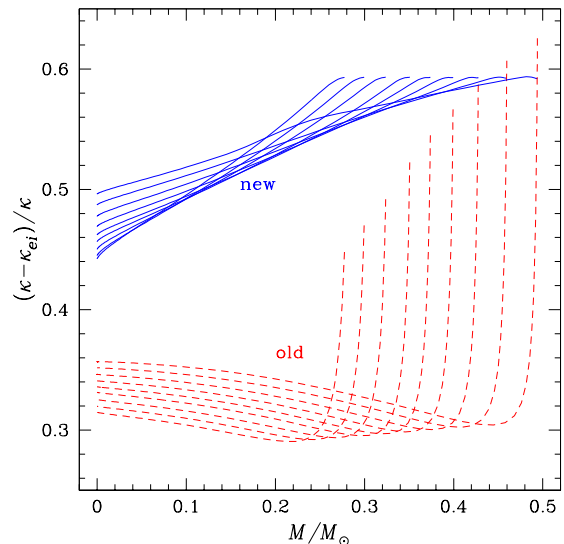


FIG. 3.— Ratio of the ee interaction opacity to the total ($ee + ei$) conductive opacity along the RGB core models of a $0.8M_\odot$ metal poor star discussed by Catelan (2005), as a function of the Lagrangian mass coordinate (in solar units). For the ei contribution to the opacity, the fitting formulae of Potekhin et al. (1999) are used together with thermal averaging according to Eqs. (11) and (12). For the ee contribution, the *solid lines* correspond to Eqs. (9), (10), and (13), and the *dashed lines* to the older theory for degenerate electrons (Urpin & Yakovlev 1980; Potekhin et al. 1999). Each curve of a series corresponds to a specific RGB stellar model, whose He core mass is equal to the value of the mass attained at the end of the curve.

- In degenerate matter, the old theory (Urpin & Yakovlev 1980) and corresponding analytical formulae (Potekhin et al. 1997, 1999) are replaced by the new theory and analytical formulae by Shternin & Yakovlev (2006) (see § 2.2.2).
- In partially degenerate and nondegenerate matter, extrapolation of the ee opacity according to model B above is replaced by the interpolation formula (13), which correctly reproduces the high-temperature asymptote (6) and minimizes differences with respect to numerical tables in the domain of weak degeneracy (see § 2.3).

Note that the latter interpolation does not concern the ei contribution to the opacity, which is calculated numerically according to Eqs. (11) and (12).

We have updated previously developed Fortran code for thermal conductivities of electron-ion plasmas in arbitrary magnetic fields available online (see footnote 7) by including ee scattering in the particular case of zero magnetic field, taking into account the recent progress in the treatment of the ee conductive opacity, summarized above. We have also updated the table of thermal conductivities of fully ionized electron-ion plasmas, calculated using this code and available at the same URL. The table covers densities ρ from 10^{-6} to 10^9 g cm $^{-3}$, temperatures T from 10^3 to 10^9 K, and ion charge numbers Z_i from 1 to 60. For convenience of potential users, the table is supplemented by an interpolation routine in Fortran.

In Fig. 3 we show the ratio of the ee interaction opacity to the total conductive opacity in the RGB core mod-

⁷ <http://www.ioffe.ru/astro/conduct/>

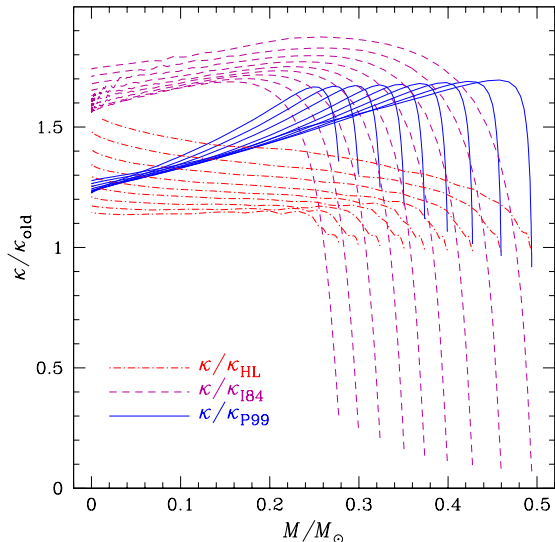


FIG. 4.— Ratio of the $ee + ei$ conductive opacity κ_c computed in this paper to previous evaluations by Hubbard & Lampe (κ_{HL} , dot-dashed lines), Itoh et al. (κ_{I84} , dashed lines), and Potekhin et al. (κ_{P99} , solid lines) for the same stellar models of Fig. 3.

els discussed by Catelan (2005). The new results (*solid lines*), which correspond to Eq. (13), are compared with the old model B (*dashed lines*, which is similar to Fig. 19 in Catelan 2005). The differences between the new and old results are caused, first, by the better treatment of ν_{ee} in the regime of partial degeneracy according to Eq. (13), which decreases the opacity at $T \gg T_F$ but increases it at $T \sim T_F$, and secondly, by the improved treatment of ν_{ee}^{deg} , reviewed in § 2.2.2, which increases the opacity at high densities. The opacity decrease is noticeable only in the outer layers of the RGB stellar models with relatively high M_{tot} , whereas the increase is overwhelming in the most of the stellar core. On the whole, in the new calculations the ee interactions play an even more important role for the physical conditions prevailing in the interiors of low-mass RGB stars than had previously been suspected (Catelan et al. 1996; Catelan 2005).

Figure 4 shows the ratio of our present conductive opacities to various approximations employed previously. One can notice values that are significantly different from unity. The difference between our results and Potekhin (1999) (solid curves) is due to the neglect of the ee scattering by the latter. In the case of the comparison with Hubbard & Lampe (1969) (dot-dashed curves) the difference is mainly due to the deficiency of their treatment of strongly coupled and relativistic plasmas, discussed above. The comparison with Itoh et al. (1984) (dashed curves) shows differences that are partly due to the ee collisions, but the most striking difference at the end of each curve (that corresponds to the boundary of the He core) occurs because $T > T_F$ there, whereas the Itoh et al. formulae are valid only for $T \ll T_F$.

3. THE EFFECT ON THE EVOLUTION OF LOW-MASS STARS

In the following we analyze the effect of our new conductive opacities on the evolution of low-mass stars. For the tests involving RGB and HB models we employed the same stellar evolution code and input physics discussed

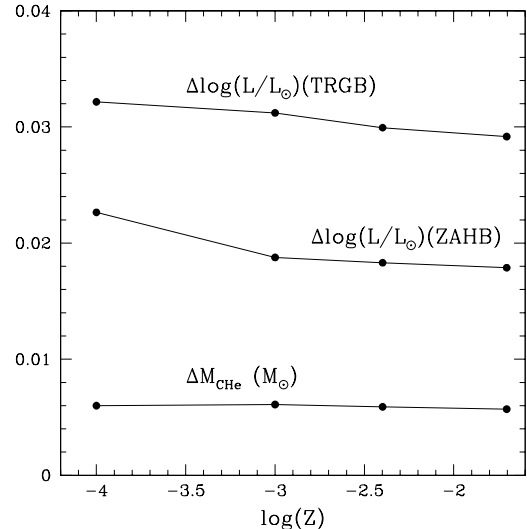


FIG. 5.— Differences in the He-core mass, RGB tip brightness and ZAHB luminosity as a function of the heavy element abundance, between stellar models computed with the ‘old’ conductive opacities by Potekhin (1999) and our new κ_c estimates (see text for details).

in Pietrinferni et al. (2004), the only difference being the use of our new conductive opacities in place of the Potekhin (1999) ones. More in detail, we have computed the evolution of the following models: i) $M_{\text{tot}} = 0.8 M_{\odot}$, $Z = 10^{-4}$, $Y = 0.245$, ii) $M_{\text{tot}} = 0.8 M_{\odot}$, $Z = 10^{-3}$, $Y = 0.246$, iii) $M_{\text{tot}} = 0.85 M_{\odot}$, $Z = 0.004$, $Y = 0.251$, and iv) $M_{\text{tot}} = 1.0 M_{\odot}$, $Z = 0.0198$, $Y = 0.2734$. This choice of initial stellar masses and chemical composition allows us to compare directly these models with the results by Pietrinferni et al. (2004), who employed the Potekhin opacities.

3.1. Evolution along the Red Giant Branch

The evolution of the models has been followed from the Zero Age Main Sequence until He ignition at the RGB tip. We have included mass loss according to the Reimers (1975) formula with $\eta = 0.4$. The new conductive opacities do not affect the morphology and location of the evolutionary tracks in the H-R diagram: as expected, only the He-core mass at the He-flash and the corresponding RGB tip brightness are modified. In Table 1 the main properties of the two sets of RGB models computed by using alternatively the ‘old’ κ_c predictions and the ‘new’ ones are summarized; Fig. 5 displays the differences of the model He-core masses and RGB tip brightness as a function of Z .

Our new κ_c values provide He-core masses at the He-flash lower than in the case when the previous κ_c calculations are used (model A described in § 2.4). The difference amounts to $0.006 M_{\odot}$, regardless of the value of Z . The reason is that the new κ_c values are larger than the older ones, thus producing a different thermal stratification in the He core. The stellar models based on the updated κ_c at the RGB tip are cooler at the center of the star but hotter at the point of the maximum off-center temperature where the He-ignition occurs. This is clearly shown by Fig. 6 (left panel) that displays the thermal stratification along the He core, at different stages

TABLE 1
SELECTED PROPERTIES OF THE MODELS AT THE RGB TIP.

version	$t_{\text{TRGB}}^{\text{a}}$	$\log(L/L_{\odot})^{\text{b}}$	$\log T_{\text{eff}}^{\text{c}}$	$\log T_{\text{c}}^{\text{d}}$	$\log \rho_{\text{c}}^{\text{e}}$	$M_{\text{cHe}}^{\text{f}}$	$M(T_{\text{max}})^{\text{g}}$	$\log T_{\text{max}}^{\text{h}}$	M_I^{i}
$0.8 M_{\odot} - Z = 0.0001 - Y = 0.245$									
new	12.49	3.2586	3.6427	7.863	6.061	0.4971	0.178	7.973	-4.085
old	12.48	3.2908	3.6411	7.870	6.079	0.5031	0.170	7.968	-4.164
$0.8 M_{\odot} - Z = 0.001 - Y = 0.246$									
new	13.69	3.3384	3.5958	7.870	6.020	0.4852	0.162	7.969	-4.147
old	13.68	3.3696	3.5946	7.877	6.039	0.4913	0.154	7.966	-4.223
$0.85 M_{\odot} - Z = 0.004 - Y = 0.251$									
new	13.63	3.3829	3.5473	7.873	5.997	0.4788	0.167	7.975	-3.933
old	13.62	3.4128	3.5453	7.880	6.015	0.4847	0.161	7.970	-3.989
$1.0 M_{\odot} - Z = 0.0198 - Y = 0.2738$									
new	12.52	3.4168	3.4822	7.874	5.954	0.4669	0.191	7.978	-2.266
old	12.50	3.4459	3.4766	7.881	5.972	0.4726	0.128	7.977	-2.239

^aAge (in Gyr) at the RGB tip.

^bLogarithm of the luminosity (in solar units) at the RGB tip.

^cLogarithm of the effective temperature at the RGB tip.

^dLogarithm of the central temperature (in K) at He ignition.

^eLogarithm of the central density (g cm^{-3}) at He ignition.

^fHe-core mass (in solar units) at He ignition.

^gLocation in mass (in solar units) of the off-center temperature maximum at the RGB tip.

^hLogarithm of the maximum off-center temperature (in K) at He ignition.

ⁱAbsolute *I*-Cousins magnitude of the RGB tip.

along the RGB, for a selected metallicity. The right panel in the same figure shows the correspondence between the various internal structures and the location of the models along the RGB in the H-R diagram.

The stellar models based on the new κ_{c} achieve the thermal conditions required for the He-ignition at a slightly higher age (see Table 1) compared to the model A mentioned above. This is because the new conductive opacities force the stellar structures to have a different temperature gradient in the He core. As a consequence, the temperature at the base of the H-burning shell is slightly lower than for models based on the old κ_{c} determinations (see data shown in Fig. 6).

The difference in He-core mass at the RGB tip causes a change of the RGB tip brightness: new models appear to be fainter by $\Delta \log(L/L_{\odot}) \approx 0.03$. This change affects distances based on the RGB tip brightness. It is well known (see, e.g., Lee et al. 1993; Salaris & Cassisi 1998) that the *I*-band (Cousins) brightness of the RGB tip (M_I^{TRGB}) is a powerful distance indicator for old, metal-poor and intermediate-metallicity stellar systems such as Local Group Dwarfs, because it is very weakly sensitive to the heavy element abundance (and age, for ages above a few Gyr). For $[M/H]$ ($[M/H] = \log(Z/X) - \log(Z/X)_{\odot}$) ranging between -2.0 and -0.6 , M_I^{TRGB} changes by about 0.15 mag. The RGB tip brightness being fixed by the He-core mass at the He-flash, any change in M_{cHe} translates into a variation in M_I^{TRGB} .

The data in Table 1 show how the new κ_{c} decreases the *I*-band brightness of the RGB tip by about 0.07 – 0.08 mag for metallicities lower than about $Z \sim 0.004$. At solar metallicity, the behavior reverses and the new estimate is brighter by ~ 0.03 mag. This reversal of the trend is entirely due to the trend of bolometric correction BC_I with T_{eff} , which overcompensates the smaller bolometric luminosity at the RGB tip. In fact, all stellar tracks based on the new κ_{c} experience the He-ignition at

fainter bolometric magnitudes and higher effective temperatures. The higher T_{eff} values are caused by the larger (of the order of $0.01 M_{\odot}$) total mass at the flash, which is a consequence of the smaller amount of mass lost along the RGB evolution, due to the shorter RGB evolutionary lifetime and lower RGB tip luminosity of the models. Because of the trend of BC_I with T_{eff} , the final value of M_I^{TRGB} gets brighter at this high metallicity.

The M_I^{TRGB} values obtained with our new opacities turn out to be within about 1σ of the empirical value obtained by Bellazzini, Ferraro, & Pancino (2001), who coupled their own detection of the RGB tip in the Galactic globular cluster ω Centauri (NGC 5139) to the cluster distance obtained by Thompson et al. (2001) from the analysis of the cluster eclipsing binary OGLEGC 17.

Before closing this section, we wish to note that the main source of change in the value of M_{cHe} when moving from the κ_{c} evaluations provided by Potekhin (1999) to our new conductive opacities is related to the inclusion of the *ee* interactions in our new treatment of conductive transport. More in detail, proper treatment of the *ee* interactions according to the fit (13), but with the old treatment of the *ee* scattering frequency in degenerate matter ν_{ee}^{deg} (Urpin & Yakovlev 1980; Potekhin et al. 1997, 1999), contributes about 70% (i.e., $\sim 0.004 M_{\odot}$) of the change in M_{cHe} . The better treatment of ν_{ee}^{deg} that takes into account the relativistic effect of exchange of transverse plasmons (see § 2.2.2) accounts for the remaining one-third of the total variation.

3.2. Evolutionary Properties during the Core He-Burning Phase

As discussed in the Introduction, any change of the He-core mass at He ignition causes a variation in the luminosity of the Zero Age Horizontal Branch (ZAHB). It is worthwhile to investigate how the change in M_{cHe} brought about by the new opacities affects the properties

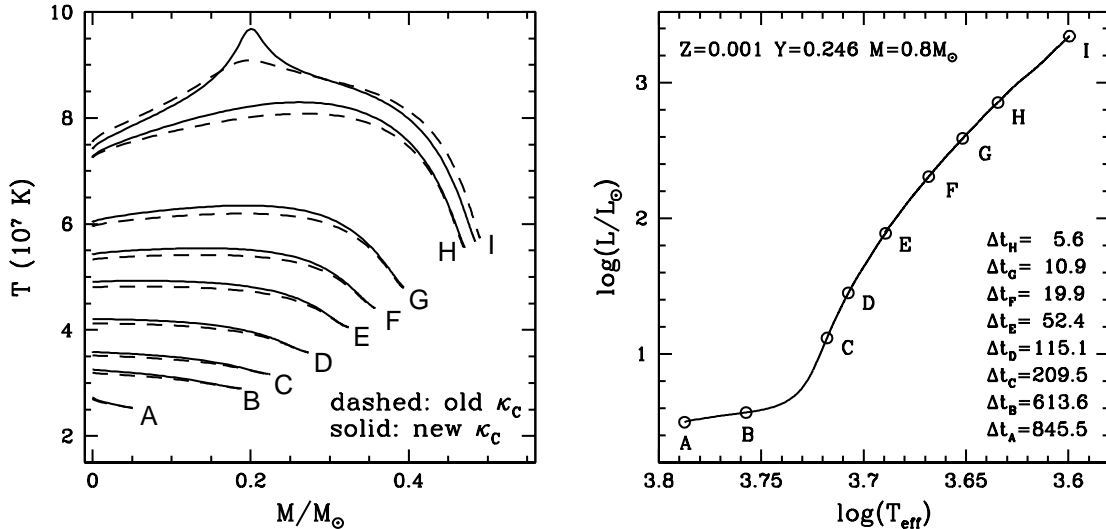


FIG. 6.— *Left panel*: thermal stratification of the He core at different stages along the RGB evolution of a $0.8 M_{\odot}$, $Z = 0.001$, $Y = 0.246$ model, computed with the ‘old’ conductive opacities by Potekhin (1999, *dashed lines*) and our new computations (*solid lines*) respectively. The hottest sequences correspond to ignition of He at the tip of the RGB. *Right panel*: location in the H-R diagram of the stellar models (labelled with capital letters) whose thermal stratification is shown in the left panel. For each model, the time (in Myr) needed to reach the He flash at the RGB tip is also listed.

of HB stellar models. To this purpose, we computed a set of HB models originated from the RGB progenitors discussed above.

We focus our attention on the HB models whose ZAHB location is at $\log(T_{\text{eff}}) = 3.85$. We choose this effective temperature value⁸ for consistency with our previous analysis on this issue.

The main properties of these models are listed in our Table 2. The ZAHB models with the updated κ_c are fainter than those based on the previous estimates, because of the lower He-core mass of the progenitor. The difference is $\Delta \log(L/L_{\odot}) \sim 0.02$ within the explored metallicity range. The corresponding V -band ZAHB brightness ($M_V(\text{ZAHB})$) of the models is reported in Table 2. The new conductive opacities cause an increase in $M_V(\text{ZAHB})$ ranging from ~ 0.06 mag at $Z = 0.0001$ down to ~ 0.04 mag at solar metallicity. This has the effect of slightly decreasing the distance to Galactic globular clusters and of systematically increasing their ages by ~ 0.7 Gyr. These changes in the globular cluster age and distance scales are within current uncertainties on these estimates (for more details, see, e.g., Recio-Blanco et al. 2005; De Angeli et al. 2005, and references therein).

As to the location in effective temperature of the ZAHB models, we have already shown that for a given RGB progenitor and for fixed mass-loss efficiency along the RGB, the total stellar mass at He ignition increases. This occurrence – combined with the decrease of the He core mass – will cause the ZAHB model location to be slightly cooler with respect to the model based on the old opacity predictions.

A consequence of the lower HB luminosity is that the evolutionary lifetime of the core He-burning phase is slightly longer, by ~ 5 –6%. Together with the

⁸ We note that this T_{eff} value cannot be considered fully representative of the average temperature in the RR Lyrae strip (see for instance, Marconi et al. 2003). However, this has no impact on the present discussion.

TABLE 2
SELECTED PROPERTIES OF HB MODELS.

version	$M_{3.85}$ ^a	$\log(L/L_{\odot})_{3.85}$ ^b	M_V ^c	t_{HB} ^d
RGB progenitor: $0.8 M_{\odot} - Z = 0.0001 - Y = 0.245$				
new	0.785	1.734	0.434	83.55
old	0.801	1.757	0.377	79.03
RGB progenitor: $0.8 M_{\odot} - Z = 0.001 - Y = 0.246$				
new	0.629	1.645	0.628	94.61
old	0.639	1.664	0.582	89.64
RGB progenitor: $0.85 M_{\odot} - Z = 0.004 - Y = 0.251$				
new	0.577	1.575	0.825	102.98
old	0.585	1.593	0.750	100.69
RGB progenitor: $1.0 M_{\odot} - Z = 0.0198 - Y = 0.2738$				
new	0.531	1.445	1.066	115.88
old	0.538	1.463	1.029	111.53

^aMass (in solar units) of the ZAHB model located at $\log T_{\text{eff}} = 3.85$.

^bLogarithm of the luminosity (in solar units) of the ZAHB model located at $\log T_{\text{eff}} = 3.85$.

^cAbsolute visual magnitude of the ZAHB model located at $\log T_{\text{eff}} = 3.85$.

^dCore He-burning lifetime (in Myr) of the HB structure with ZAHB location at $\log T_{\text{eff}} = 3.85$.

lower luminosity of the RGB tip and the fainter ZAHB, this might affect the theoretical calibration of the R -parameter, i.e., the ratio of the number of HB stars to the number of RGB objects brighter than the ZAHB level (Iben 1968) that is often used as an indicator of the initial He abundance of Galactic globular clusters. Recently, Cassisi, Salaris, & Irwin (2003) and Salaris et al. (2004) have derived a new calibration of R (using the Potekhin 1999 conductive opacities) that, applied to a large and homogeneous database of empirical values for Galactic globulars, provides an initial He-abundance in very good agreement with the determination based on recent analysis of Cosmic Microwave Background fluctuations and

Big Bang nucleosynthesis predictions (see Spergel et al. 2006 and references therein). Here we have estimated the value of the R parameter based on the models presented in the previous sections and compared the results with ones based on the Potekhin opacities. The use of the new κ_c increases the HB lifetime (t_{HB}) by $\sim 5\%$, but the time spent by the RGB progenitor at luminosities higher than the ZAHB level also increases by $\sim 3.5\%$. The net effect is that, for a fixed initial chemical composition, the value of R changes by just $+0.03$ ($\sim 2\%$). The dependence of the R -parameter on the He content is $\delta R/\delta Y \sim 10$ (see Cassisi et al. 2003) and therefore the change of the R calibration caused by the new κ_c would lead to a variation by only 0.003 of the estimated initial He content of the Galactic globular cluster system. This means that the reliability of the R -parameter calibration presented by Cassisi et al. and Salaris et al. is not seriously affected by the revised conductive opacities.

3.3. Very Low-Mass Stars and White Dwarfs

In very low-mass (VLM) stars, i.e. structures with mass lower than $\sim 0.3\text{--}0.4 M_{\odot}$, the temperature is of the order of the electron Fermi temperature. More in detail, considering $T/T_F \approx 3.31 \times 10^{-6} T(\mu_e/\rho)^{2/3}$ together with values of temperature and density characteristic of the interiors of VLM stars, one obtains $T/T_F \sim 1 - 2$. This means that the VLM stellar interiors are under conditions of partial electron degeneracy, the degeneracy level strongly decreasing with the total mass. Taking into account such circumstantial evidence, we decided to test the impact of the new opacity estimates on the structure and evolution of VLM stars. We adopted the same evolutionary code and physical inputs as in Cassisi et al. (2000) but including our new conductive opacities. We computed VLM stellar models in the mass range $0.09 - 0.15 M_{\odot}$ for a metallicity $Z = 0.001$. A close comparison with the corresponding evolutionary models provided by Cassisi et al. (2000), based on the Itoh et al. (1993) conductive opacities, shows that – at least in the considered range of stellar mass – there are negligible differences between the two sets of stellar models concerning both the structural properties and evolutionary lifetimes.

The extremely degenerate cores of white dwarfs are properly covered by the Itoh et al. and Yakovlev et al. opacities, whereas the Hubbard & Lampe (1969) opacities are not adequate in this regime (see, e.g., Prada Moroni & Straniero 2002). However, it is well known (see, e.g., Hansen 1999; Salaris et al. 2000; Prada Moroni & Straniero 2002) that neither the Itoh et al. nor the Hubbard & Lampe conductive opacities can completely cover the He-envelopes of white dwarfs during their entire cooling phase. A solution generally used (see, e.g., the models by Hansen 1999; Salaris et al. 2000) is to employ the Itoh et al. (or Yakovlev et al.) opacities, supplemented outside their range of validity (e.g., when the matter is only weakly degenerate) by the Hubbard & Lampe data. Given that the different opacity sources are not based on the same assumptions and input physics (see §§ 1, 2) their matching in the regime of weak degeneracy is sometimes problematic.

It should be stressed that the Potekhin et al. (1999) opacities, calculated a few years ago and aimed especially at white dwarf and neutron star applications, have

already superseded the older results of Itoh et al., as explained in §2. Nevertheless, even the Potekhin et al. opacities should be corrected following the improvement of the treatment of the ee scattering contribution described in §§ 2.2.2 and 2.3.

Here we test the impact of the new opacities described in §2 and available at the URL referenced in footnote 7 on the cooling timescale of white dwarfs. We emphasize that the new calculations adequately cover the whole white dwarf structure during its cooling sequence. We employed the same code and input physics as in Salaris et al. (2000) to compute the cooling evolution of a $0.54 M_{\odot}$ and a $1.0 M_{\odot}$ DA white dwarf with a pure carbon core (the thickness of the He and H envelope layers is as in Salaris et al. 2000) using both our new opacities and the combination of Itoh et al. and Hubbard & Lampe (1969) opacities mentioned before. The mass-radius relationship is unchanged, and the cooling times at a given luminosity turn out to be almost exactly the same, irrespective of the opacities used. The maximum differences are of the order of just 1% (the cooling times obtained with the new opacities being longer) when $\log(L/L_{\odot}) < -5.0$ and the cooling ages are above 14 Gyr.

4. SUMMARY

We have reviewed the basic theory to estimate the electron-conduction opacity for the stellar matter, and discussed limitations and shortcomings of the existing calculations that are employed in stellar evolution modelling. We present new results that can be applied to both partial (e.g., in the cores of RGB stars, envelopes of white dwarfs) and high degeneracy (e.g., white dwarf cores) regimes, for an arbitrary chemical composition. Our results update the previous calculations by Hubbard & Lampe (1969), Itoh and coworkers (e.g., Itoh et al. 1983, 1984, 1993), and Yakovlev and coworkers (e.g., Potekhin et al. 1999; Potekhin 1999; Shternin & Yakovlev 2006), extensively used in the literature. They improve upon Hubbard & Lampe (1969) by including an updated treatment of both the ei scattering and the ee scattering for strongly coupled and relativistic plasmas, and are not restricted to the specific mixtures published by Hubbard & Lampe. Differences with Itoh and coworkers are mainly due to their neglect of the ee scattering, inaccurate treatment of the ei scattering at $\Gamma \sim 100 - 200$, and the fact that their results do not extend to the regimes of partial degeneracy ($T > T_F$) and weak ion coupling ($\Gamma < 1$). Differences with Potekhin (1999) are essentially due to his neglect of the ee scattering. Compared to the latest results of Yakovlev’s group (Potekhin et al. 1999; Shternin & Yakovlev 2006), our new opacities differ essentially in the extension of the ee scattering results to the regime of partial degeneracy. We compared our new computations with the aforementioned sets of opacities in the temperature-density regime of RGB star cores, and found non-negligible differences. On the whole, the Hubbard & Lampe (1969) results are the most similar to ours in the RGB cores, the maximum differences being equal to $\sim 50\%$ in the central regions of the cores.

The effect of using our new opacities for RGB and HB calculations instead of the Potekhin (1999) data is to decrease the bolometric luminosity of the RGB tip and the ZAHB by $\Delta \log(L/L_{\odot}) \sim 0.03$ and $\Delta \log(L/L_{\odot}) \sim 0.02$, respectively. The He-core masses at the RGB tip are

decreased by $\sim 0.006 M_{\odot}$, the total RGB evolutionary timescales are almost unchanged, but the time spent along the RGB above the HB increases by $\sim 3\%$, and the HB evolution is longer by $\sim 5\%$. The calibration of the R -parameter as a function of Y remains almost unchanged.

When our new opacities are applied to white dwarf models, the resulting mass-radius relationship and cooling times are essentially unchanged compared to the results obtained employing the combination of Itoh and Hubbard & Lampe (1969) opacities that until now was needed to cover the whole white dwarf structures. The

impact on Main Sequence models of very-low-mass stars is also negligible.

A.P. is grateful to Dima Yakovlev, Andreas Reisenegger, Peter Shternin, and Stephanie Hansen for useful discussions and remarks. The work of A.P. is supported in part by FASI (Rosnauka) grant NSh-9879.2006.2, by RFBR grants 05-02-16245 and 05-02-22003, and by the Visiting Professors Program of Pontificia Universidad Católica de Chile. M.C. acknowledges support by Proyecto FONDECYT Regular No. 1030954.

REFERENCES

- Baiko, D. A., & Yakovlev, D. G. 1995, *Astron. Lett.*, 21, 702
 Baiko, D. A., Kaminker, A. D., Potekhin, A. Y., & Yakovlev, D. G. 1998, *Phys. Rev. Lett.*, 81, 5556
 Barriga-Carrasco, M. D., & Potekhin, A. Y. 2006, *Laser and Particle Beams*, 24, 553
 Bellazzini, M., Ferraro, F. R., & Pancino, E., 2001, *ApJ*, 556, 635
 Braginskii S. I. 1958, *Sov. Phys. JETP*, 6, 358
 Brown, E. F., Bildsten, L., & Chang, P. 2002, *ApJ*, 574, 920
 Carson, T. R. 1976, *ARA&A*, 14, 95
 Cassisi, S., Castellani, V., Ciarcelluti, P., Piotto, G., & Zoccali, M. 2000, *MNRAS*, 315, 679
 Cassisi, S., Salaris, M., & Irwin, A. W. 2003, *ApJ*, 588, 852
 Castellani, V., & Degl'Innocenti, S. 1999, *A&A*, 344, 97
 Catelan, M. 2005, in *Resolved Stellar Populations*, ed. D. Valls-Gabaud & M. Chávez (San Francisco: ASP), in press (astro-ph/0507464)
 Catelan, M., de Freitas Pacheco, J. A., & Horvath, J. E. 1996, *ApJ*, 461, 231
 Chabrier, G., & Baraffe, I. 2000, *ARA&A*, 38, 337
 De Angeli, F., Piotto, G., Cassisi, S., Busso, G., Recio-Blanco, A., Salaris, M., Aparicio, A., & Rosenberg, A. 2005, *AJ*, 130, 116
 Flowers E., & Itoh, N. 1976, *ApJ*, 206, 218
 Flowers E., & Itoh, N. 1979, *ApJ*, 230, 847
 Flowers E., & Itoh, N. 1981, *ApJ*, 250, 750
 Gnedin, O. Y., Yakovlev, D. G., & Potekhin, A. Y. 2001, *MNRAS*, 324, 725
 Hansen, B. M. S. 1999, *ApJ*, 520, 680
 Heiselberg, H., & Pethick, C. J. 1993, *Phys. Rev. D*, 48, 2916
 Hubbard, W. B. 1966, *ApJ*, 146, 858
 Hubbard, W. B., & Lampe, M. 1969, *ApJS*, 18, 297
 Iben, I. Jr. 1968, *Nature*, 220, 143
 Itoh, N., & Kohyama, Y. 1993, *ApJ*, 404, 268; erratum: 1994, *ApJ*, 420, 943
 Itoh, N., Mitake, S., Iyetomi, H., & Ichimaru, S. 1983, *ApJ*, 273, 774
 Itoh, N., Kohyama, Y., Matsumoto, N., & Seki, M. 1984, *ApJ*, 285, 758
 Itoh, N., Hayashi, H., & Kohyama, Y. 1993, *ApJ*, 418, 405; erratum: 1994, *ApJ*, 436, 418
 Lampe, M. 1968, *Phys. Rev.*, 174, 276
 Lee, M.G., Freedman, W., & Madore, B.F., 1993, *ApJ*, 417, 553
 Marconi, M., Caputo, F., Di Criscienzo, M., & Castellani, M. 2003, *ApJ*, 596, 299
 Marshak, R. E. 1940, *ApJ*, 92, 321
 Mitake, S., Ichimaru, S., & Itoh, N. 1984, *ApJ*, 277, 375
 Pietrinferni, A., Cassisi, S., Salaris, M. & Castelli, F. 2004, *ApJ*, 612, 168
 Potekhin, A. Y. 1999, *A&A*, 351, 787
 Potekhin, A. Y., & Chabrier, G. 2000, *Phys. Rev. E*, 62, 8554
 Potekhin, A. Y., & Yakovlev, D. G. 1996, *A&A*, 314, 341
 Potekhin, A. Y., Chabrier, G., & Yakovlev, D. G. 1997, *A&A*, 323, 415
 Potekhin A. Y., Baiko D. A., Haensel P., & Yakovlev D. G. 1999, *A&A*, 346, 345
 Prada Moroni, P., & Straniero, O. 2002, *ApJ*, 581, 585
 Raikh, M. E., & Yakovlev, D. G. 1982, *Ap&SS*, 87, 193
 Recio-Blanco, A., Piotto, G., de Angeli, F., Cassisi, S., Riello, M., Salaris, M., Pietrinferni, A., Zoccali, M., Aparicio, A. 2005, *A&A*, 432, 851
 Reimers, D. 1975, *Mem. Soc. R. Sci. Liege*, 8, 369
 Renzini, A., & Fusi Pecci, F. 1988, *ARA&A*, 26, 199
 Salaris, M., & Cassisi, S., 1998, *MNRAS*, 298, 166
 Salaris, M., García-Berro, E., Hernanz, M., Isern, J., & Saumon, D. 2000, *ApJ*, 544, 1036
 Salaris, M., Riello, M., Cassisi, S., & Piotto, G. 2004, *A&A*, 420, 911
 Salaris, M., Cassisi, S., & Weiss, A. 2002, *PASP*, 114, 375
 Shternin, P. S., & Yakovlev, D. G. 2006, *Phys. Rev. D*, 74, 043004
 Spiegel, D. N., Bean, R., Doré, O., et al. 2006, *ApJ*, submitted (astro-ph/0603449)
 Spitzer L., Jr. 1962, *Physics of Fully Ionized Gases*, 2nd revised edition (Wiley: New York)
 Spitzer, L., Jr., & Härm, R. 1953, *Phys. Rev.*, 89, 977
 Thompson, I. B., Kałużny, J., Pych, W., Burley, G., Krzemnski, W., Paczynski, B., Persson, S. E., & Preston, G. W. 2001, *AJ*, 121, 3089
 Urpin, V. A., & Yakovlev D. G. 1980, *Soviet Ast.*, 24, 126
 Ventura, J., & Potekhin, A. Y. 2001, in *The Neutron Star – Black Hole Connection*, ed. C. Kouveliotou, J. van Paradijs, & J. Ventura, NATO ASI Ser. C, vol. 567 (Dordrecht: Kluwer), 393
 Yakovlev, D. G. 1987, *Soviet Ast.*, 31, 347
 Yakovlev, D. G., & Urpin, V. A. 1980, *Soviet Ast.*, 24, 303
 Young, D. A., Corey, E. M., & DeWitt, H. E. 1991, *Phys. Rev. A*, 44, 6508
 Ziman, J. M. 1960, *Electrons and Phonons* (Oxford: Oxford University Press)